

The Effects of Surface Wettability on Droplet Fingering

C. Stanley¹, R. Jackson¹, N. Karwa¹ and G. Rosengarten¹

¹School of Aerospace, Mechanical and Manufacturing Engineering
 RMIT University, Melbourne Australia 3053, Australia

Abstract

In this paper high speed visualisation has been used to investigate the effects of surface wettability on the droplet impingement and fingering behaviour. Three surfaces have been studied: a reference surface with contact angle $\theta = 90^\circ$, a hydrophilic surface with $\theta = 15^\circ$ and a hydrophobic surface with $\theta = 165^\circ$. Droplet Weber numbers (We) ranging from 50 to 250 were studied. The reference surface showed no fingering across the range of Weber numbers tested. Fingering was found to occur on the hydrophilic surface for $We > 150$, whereas the hydrophobic surface exhibited fingering for $We > 100$. Above these thresholds the observed number of fingers around a droplet was found to be consistent between the surfaces.

Introduction

Droplet impingements on solid surfaces are of technical interest in a wide variety of areas, such as ink-jet printing, spray painting, internal combustion engines and spray cooling [1]. However, despite the wide spread application the droplet impact and breakup phenomenon is not fully understood. The dynamics of the fluid droplet after impact are driven by an interplay between the kinetic energy and the surface tension of the droplet. Upon impact a droplet expands to form a thin cylindrical disk known as the lamella [2]. Under certain conditions perturbations on the surface of the lamella grow and extend radially from the lamella, in what is termed ‘fingers’ [3]. Once formed, surface and fluid properties (Re , We and surface wettability) dictate whether these fingers detach from the lamella, forming satellite droplets, or remain attached to the main droplet.

Previous experiments by the current authors have shown that heat transfer rates from single droplet impingement upon hydrophilic surfaces exceed those for hydrophobic surfaces [4]. However, droplets remain pinned to the hydrophilic surface reducing the cooling effectiveness of successive droplets. Similarly, satellite droplets shed during high inertia impingement on superhydrophobic surfaces prevents effective clearing of the surface for additional droplet impingement cooling. With this in mind, the current study served as a precursor to droplet chain heat transfer experiments, and sought to identify the threshold Weber number for which fingering occurs yet total droplet retraction is possible. High-speed photography was used to investigate the influence of surface wettability and Weber number on the fingering and breakup properties of droplets impacting a dry surface with normal incidence.

Experimental Setup

Figure 1 shows a general schematic of the experimental setup. Liquid water droplets were formed using a manually actuated syringe fitted with a 30 gauge needle (OD 0.31 mm, ID 0.16 mm) aligned vertically above the test surface. The Weber number of a spherical droplet is defined to be the dimensionless quantity

$$We = \frac{\rho v^2 D_0}{\gamma} \quad (1)$$

where ρ is the fluid density, v is the droplet velocity at impact, D_0 is the droplet diameter and γ is the surface tension. Droplet Weber number were varied between 50 and 250 by adjusting the droplet fall height, with all other parameters remaining constant.

A Phantom v1610 high-speed camera coupled to a microscope was used to image the impingement phenomenon from directly beneath the surface. The camera was configured to record at 16000 fps. Timing of the image acquisition was controlled using a software threshold detection setting coupled to the cameras recording buffer.

The surface wettability was varied by using three different test surfaces: a clear plastic plate (contact angle, $\theta = 90^\circ$), a glass microscope slide with a superhydrophobic coating ($\theta = 165^\circ$) and a glass microscope slide with a hydrophilic coating ($\theta = 15^\circ$).

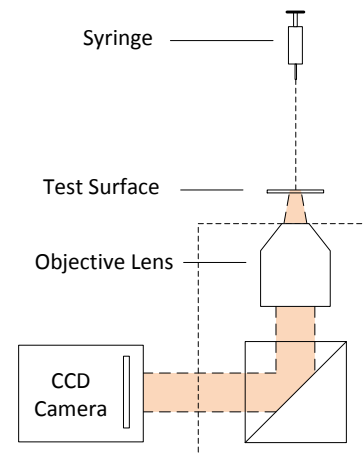


Figure 1. A general schematic of the experimental setup.

The superhydrophobic coating was comprised of a mixture of silica nanoparticles (Evonik), dimethylsiloxane polymer (Gelest) and methyltrimethoxysilane (Sigma-Aldrich) as the linking agent. This is produced and applied to the silicon wafers by the methods described in [5]. The hydrophilic coating was prepared in the same way, except that tetraethoxysilane is used as the linking agent with an ethoxylated siloxane polymer. The surface roughness of the superhydrophobic surface was measured to have an RMS value of 308 nm and a roughness ratio of 1.5 [5].

Contact angle measurements were taken for each of the surfaces using images of sessile droplets sitting on the surface. The image of the droplet was processed in Matlab by firstly extracting the pixels representing the droplet from the surrounding image, then drawing a line tangent to the first five pixels that described the curvature of the top of the droplet. The maximum error for this process is for contact angles close to 90° , where the error is

$\pm 5.5^\circ$. For superhydrophobic ($\theta > 165^\circ$) and hydrophilic ($\theta < 15^\circ$), the error is less than $\pm 0.4^\circ$.

The spatial resolution of the images was determined by placing a ruler scale on focal plane of the microscope. At Weber numbers beyond 50 the droplet would expand beyond the visible region on the microscope objective. In these instances the portion of the droplet visible throughout the expansion/contraction process was used for analysis. Improvements to the optical setup are currently being implemented and will be used for the forthcoming experiments.

Results

Visualisation of the droplet impact

Figure 2 shows a typical droplet impact image sequence for all three surface types at $We = 50$. At this Weber number the effects of surface tension are dominant and the general appearance of the droplets was similar for all three surfaces. On all surfaces the droplets expanded smoothly with no noticeable peripheral perturbations. For the normal surface ($\theta = 90^\circ$) the droplet reached maximum dimension and then began to very slowly recoil due to surface tension drawing the fluid back to an equilibrium diameter.

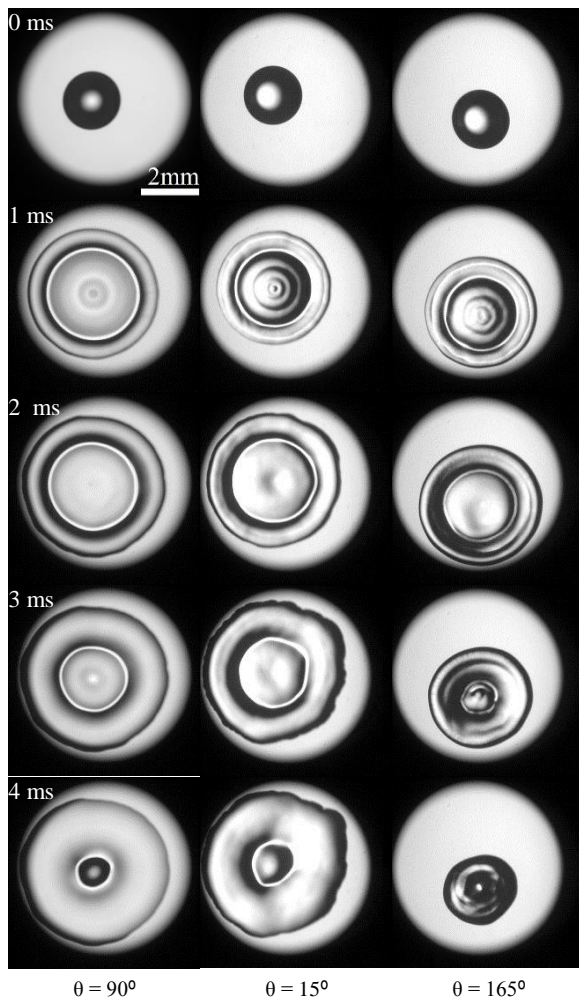


Figure 2. Droplet impact sequence for $We = 50$.

However, for the hydrophilic surface the droplet was observed to continue to spread gradually after the initial expansion, due to the wettability of the surface. Sometimes this spreading was observed to be non-symmetrical; most likely the consequence of the fluid adhering to surface imperfections. Contrary to this, the

droplet reached maximum spread diameter then uniformly recoiled to a central droplet for the hydrophobic surface.

As the Weber number of the droplets was increased the differences in the droplet behaviour became more pronounced. At $We = 100$, the normal surface droplet behaved as previously described. The droplet on the hydrophilic surfaces begins to exhibit slight circumferential rippling. These are very minor and do not constitute fingers. For the hydrophobic surface however, the outer circumference of the expanding droplets has well defined, relatively evenly spaced oscillations. As the droplet expands a number of adjacent protrusions can be seen to merge together radially. This effect increases the volume of the liquid in the protrusions extending from the lamella. A small number of the protrusions form fingers. As the droplet begins to contract the liquid in the regions between these fingers starts to retract before the liquid in the fingers themselves. This delay accentuates the shape of the finger and causes 'necking'. In some instances, should the finger extend far enough from the main droplet volume, surface tension acts to sever the 'neck' of the finger and creates a satellite droplet. However, as this pinching off of droplets occurs after the droplet recoil has commenced the shed droplet has some inward inertia and tends to eventually merge with the main droplet.

A typical droplet impact sequence for $We = 150$ on the hydrophilic surface is shown in figure 3. At this Weber number the surface perturbations around the periphery of the lamella for the hydrophilic surface have grown in size. The circumferential spacing of these perturbations appeared fairly uniform, however the size of the protrusions were not uniform. Typically only a small number of these ripples grew into full fingers. The minimal length of the fingers, combined with the wettability of the surface ensures no 'necking' of the fingers occurs. Following expansion to a maximum spreading radius the liquid within the droplet begins to contract and a pulse of liquid can be inferred from the capillary waves travelling radially inwards. The outer periphery of the droplet appears to contract slightly before the liquid becomes pinned in place via the forces of surface tension along the three phase contact line. From this point the lamella, together with the protruding fingers, becomes locked in position. The liquid within the droplet can be seen to oscillate radially as the inertial energy of the initial expansion is dissipated.

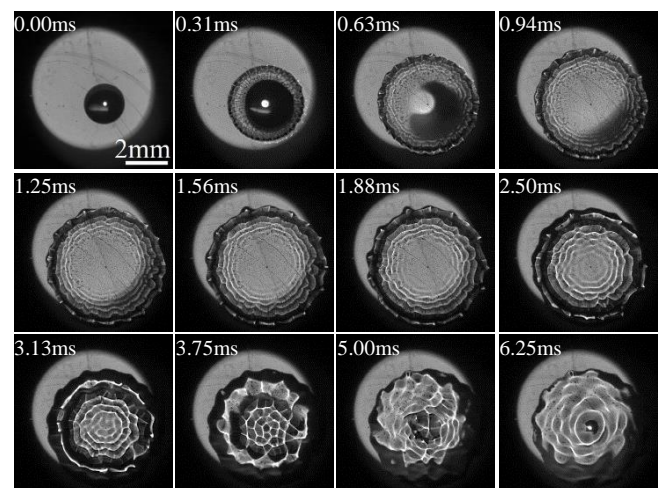


Figure 3. Droplet impact sequence for hydrophilic surface at $We = 150$.

Figure 4 shows a droplet impact sequence on the hydrophobic surface at $We = 150$. The fingers can be seen to form evenly around the periphery of the droplet immediately upon expansion. As the droplet nears the maximum expansion the fingers were observed to continue to expand causing necking to occur. In some cases the finger has sufficient radial inertia to break free

from the lamella during expansion, resulting in satellite droplets. In most cases, however, as the main droplet just begins to retract the necking of the fingers is accentuated, causing pinching off of the finger extremity into droplets. These droplets have sufficient momentum that they generally continue to expand slightly away from the impact point. The remainder of the droplet recoils under the influence of liquid surface tension and forms a single central droplet.

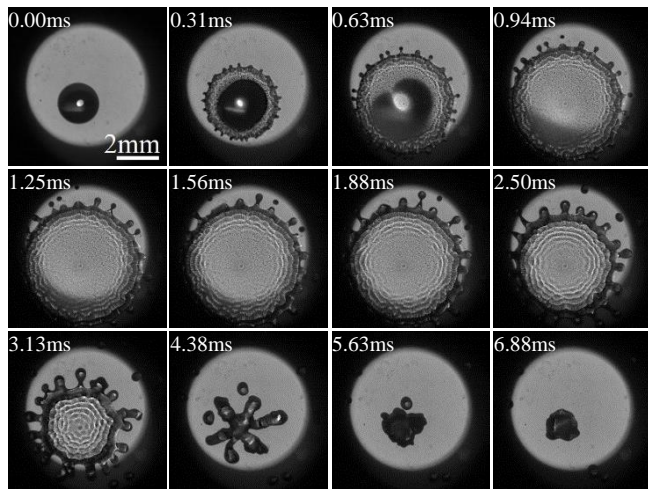


Figure 4. Droplet impact sequence for hydrophobic surface at $We = 150$.

As the Weber number was increased further to $We = 200$ the patterns observed for lower We were further heightened. The normal surface continued to exhibit no fingering of the droplet; with the lamella expanding, reaching a maximum radius and then very slowly recoiling to a central droplet. For the hydrophilic surface, the protrusions around the circumference of the droplet now form fingers which are relatively evenly spaced and are roughly uniform in length. As was the case as $We = 150$, the lamella and fingers expand to a maximum size before the liquid surface tension overcomes the radial inertia and the liquid rebounds. At this point the three phase contact line is pinned due to the wettability of the surface and the liquid travels radially inward creating complex wave patterns on the surface of the droplet. The fingers, which originally appeared rounded at their tips become more pointed in appearance as the liquid from within their volume is withdrawn by the actions of liquid surface tension.

For the hydrophobic surface well developed fingers are present by the time the droplet has expanded along the surface beyond the free fall droplet radius (first visible expansion frame). These fingers expand at a quicker rate than the lamella causing satellite droplets to be shed from the main lamella before the droplet has reached its maximum expansion radius. After the original finger is pinched off, the portion of the finger remaining intact with the droplet lamella continues to grow, expanding faster than the main droplet, and form a secondary finger. The lamella reaches a maximum radius and begins to contract as the secondary fingers stop expanding. This retraction of the droplet causes necking of the secondary fingers and eventual pinching off of a second satellite droplet. If this secondary shedding occurs sufficiently into the droplet retraction process then there is a small degree of inward inertia imparted on the secondary satellite droplet. In this case the secondary satellite droplets slowly migrate and coalesce with the main droplet, which has recoiled under the influence of liquid surface tension.

A droplet impact sequence at $We = 250$ for the hydrophilic surface is shown in Figure 5. The fingers protruding from the droplet are immediately obvious as the droplet commences its expansion. A small number of fingers around the periphery,

which appear to have formed very early in the expansion, protrude further than the adjacent fingers. The rounded ends of the fingers appear to expand at a faster rate than either the lamella or the neighbouring fingers. This causes necking and eventually satellite droplets are shed. The remaining fingers expand at a similar rate to the lamella, reach a maximum radius and then are pinned in position by the wettability effects.

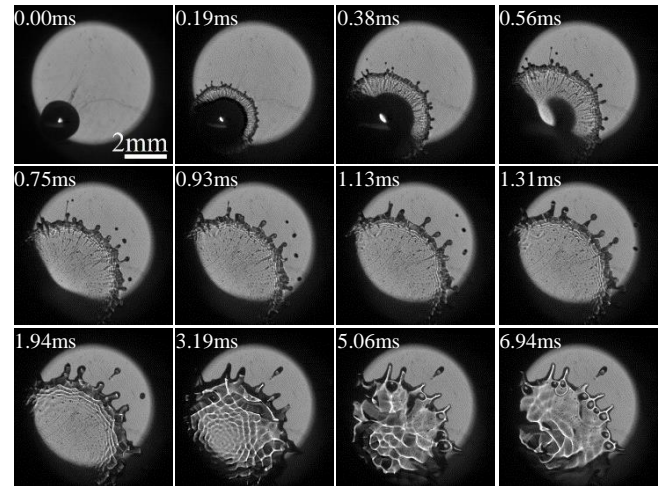


Figure 5. Droplet impact sequence for hydrophilic surface at $We = 250$.

As for the lower Weber numbers, the shape of the pinned fingers becomes more pointed as the liquid within the droplet recoils. Interestingly, occasionally the surface of the lamella was seen to rupture in the regions between two fingers near the maximum radius. This was thought to be caused by the oscillations of the droplet surface causing the liquid film to become too thin to maintain continuous coverage. The top surface of the liquid ruptures, but the surface tension force along the three phase contact line holds the liquid in place, forming circular patterns, as shown in Figure 6.

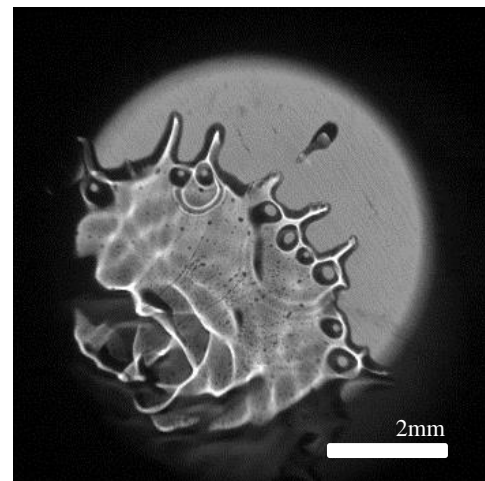


Figure 6. Droplet surface rupturing due to surface recoiling and thinning of the droplet film for a hydrophilic surface at $We = 250$, at $t = 6.94$ ms after droplet impingement.

A droplet impact sequence at $We = 250$ for the hydrophobic surface is shown in Figure 7. The additional inertial force at this weber number enhances the formation of satellite droplets. The equally spaced radial fingers, which can be seen immediately on the droplet periphery, each shed a droplet at approximately the mid-point of the expansion. These shed droplets have a high radial velocity and are projected well beyond the maximum spread radius. The fingers from which these droplets have come then continue to grow and a secondary satellite droplet is shed as the droplet approaches maximum expansion. It is common to see

adjacent fingers merging together, resulting in a longer more pronounced finger. Occasionally this occurs just after the fingers have shed their second satellite droplets. The recoiling of the droplet then causes necking in the merged finger and a third satellite droplet can shed from the lamella. Typically these are drawn towards the main droplet and coalesce.

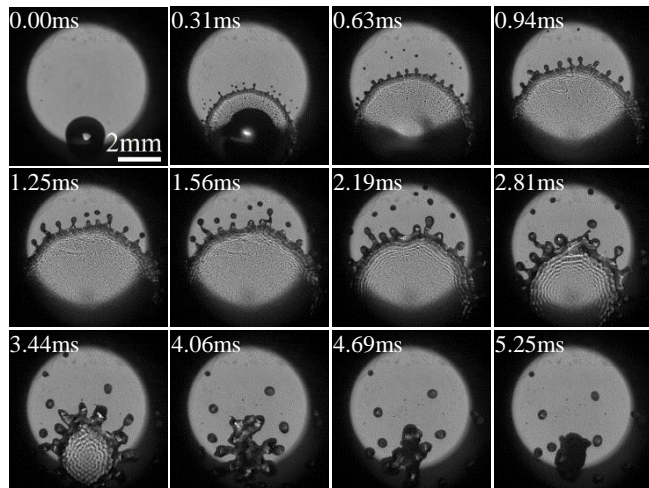


Figure 7. Droplet impact sequence for hydrophobic surface at $We = 250$.

Fingering Threshold

Table 1 presents a summary of the conditions for which fingering was observed. As previously mentioned fingering was not observed on the normal surface for any Weber number. Although fingers were occasionally seen to form on the hydrophilic surface for Weber numbers as low as 150 they were not common. With this in mind the current results suggest Weber numbers in excess of 150 are required for droplet fingering on hydrophilic surfaces. Droplets were seen to generate fingers on the hydrophobic surface for Weber numbers greater than 100. The average number of fingers around the periphery of 3 droplets for each surface was averaged and is presented in Figure 8.

We	Fingering Observed (Y/N)		
	$\theta = 15^\circ$	$\theta = 90^\circ$	$\theta = 165^\circ$
50	N	N	N
100	N	N	N
150	Y	N	Y
200	Y	N	Y
250	Y	N	Y

Table 1. Summary of conditions for which droplet fingering was observed for the three different surface wettabilities.

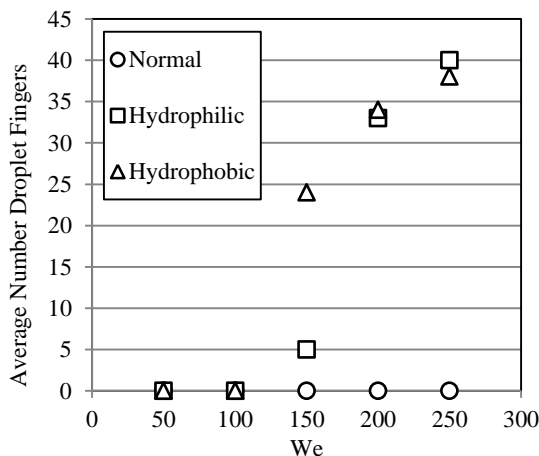


Figure 8. Average number of fingers formed per droplet.

It can be seen that despite the differences in the droplet shedding behaviour and droplet recoil after expansion, the number of fingers on the hydrophilic and hydrophobic surfaces was essentially constant beyond the threshold of occurrence ($We = 150$).

Conclusions

Droplet impingement experiments have been conducted across a range of Weber numbers from 50 to 250 to investigate the influence of surface wettability on droplet fingering. A hydrophilic and hydrophobic surface with contact angles of $\theta = 15^\circ$ and $\theta = 165^\circ$ respectively, were prepared by coating glass slides. A plastic surface with contact angle was used as a reference. High speed imagery revealed no fingering to occur for the reference surface for any of the Weber numbers tested. For the hydrophilic surface fingers were observed at $We > 150$, whereas for the hydrophobic surface fingers were seen to occur for $We > 100$. Once the droplet weber number exceeded the threshold for finger formation there was a comparable number of fingers seen on both the hydrophilic and hydrophobic surfaces. The wettability of the surface was shown to pin the droplet on the hydrophilic surface and prevent droplet retraction. For the hydrophobic surface the expanded droplet is retracts under the action of liquid surface tension.

Satellite droplets were shown to be shed from the fingers around the periphery of the droplet for both the hydrophilic and hydrophobic surfaces; however this occurs more frequently on the hydrophobic surface. The number of satellite droplets shed was seen to increase with increasing Weber number.

References

- [1] Yoon, S.S., Jepsen, R.A., James, S.C., Liu, J. & Aguilar, G., Are Drop-Impact Phenomena Described by Rayleigh-Taylor or Kelvin-Helmholtz Theory? *Drying Technology*, 2009, 27(3), 316-321.
- [2] Thoroddsen, S. & Sakakibara, J., Evolution of the Fingering Pattern of an Impacting Drop, *Physics of Fluids*, 1998, 10(6), 1359-1374.
- [3] Yarin, A., Drop Impact Dynamics: Splashing, Spreading, Receding, Bouncing..., *Annu. Rev. Fluid Mech.*, 2006, 38, 159-192.
- [4] Jackson, R.G., Kahani, M., Karwa, N., Wu, A., Lamb, R., Taylor, R. & Rosengarten, G., Effect of Surface Wettability on Carbon Nanotube Water-Based Nanofluid Droplet Impingement Heat Transfer, in *Journal of Physics: Conference Series*, 525(1), 2014, 012024.
- [5] Rosengarten, G., Tetuko, A., Li, K.K., Wu, A. & Lamb, R., The Effect of Nano-Structured Surfaces on Droplet Impingement Heat Transfer, in *ASME 2011 International Mechanical Engineering Congress and Exposition*, 2011, 1029-1036.